AD_____

Award Number:
W81XWH-10-1-0651

TITLE:
Motor Cortex Stimulation Reverses Maladaptive Plasticity Following Spinal Cord Injury

PRINCIPAL INVESTIGATOR:
Radi Masri, DDS, MS, PhD

CONTRACTING ORGANIZATION:
UNIVERSITY OF MARYLAND
BALTIMORE, MD 21201-1531

REPORT DATE:
September 2012

TYPE OF REPORT:
Annual Report

PREPARED FOR: U.S. Army Medical Research and Materiel Command
Fort Detrick, Maryland 21702-5012

REPORT DOCUMENTATION PAGE

Form Approved
OMB No. 0704-0188

1. REPORT DATE *(DD-MM-YYYY)*	**2. REPORT TYPE**	**3. DATES COVERED** *(From - To)*
01-09-2012	Annual Report	31 Aug 2011-31 Aug 2012

4. TITLE AND SUBTITLE
Motor Cortex Stimulation Reverses Maladaptive Plasticity Following Spinal Cord Injury

5a. CONTRACT NUMBER

5b. GRANT NUMBER
W81XWH-10-1-0651

5c. PROGRAM ELEMENT NUMBER

6. AUTHOR(S)

Radi Masri, DDS, MS, PhD

E-Mail: rmasri@umaryland.edu

5d. PROJECT NUMBER

5e. TASK NUMBER

5f. WORK UNIT NUMBER

7. PERFORMING ORGANIZATION NAME(S) AND ADDRESS(ES)
University of Maryland
Baltimore, MD 21201-1531

8. PERFORMING ORGANIZATION REPORT NUMBER

9. SPONSORING / MONITORING AGENCY NAME(S) AND ADDRESS(ES)
US Army Medical Research and Material Command
Fort Detrick, Maryland
21702-5012

10. SPONSOR/MONITOR'S ACRONYM(S)

11. SPONSOR/MONITOR'S REPORT NUMBER(S)

12. DISTRIBUTION / AVAILABILITY STATEMENT

Approved for public release; distribution unlimited

13. SUPPLEMENTARY NOTES

14. ABSTRACT

The majority of patients with spinal cord injury (SCI) develop intractable chronic neuropathic pain that is resistant to conventional pharmacologic treatments. An alternative and potentially effective modality of treatment—motor cortex stimulation (MCS)—offers hope for these patients. The purpose of this application is to elucidate the neurobiological basis of reduced pain following MCS. We propose that *MCS reverses hyperalgesia by enhancing the activity in the GABAergic nucleus zona incerta (ZI), and therefore inhibiting pain processing in the posterior thalamus (PO).* Using single cell extracellular electrophysiological recordings from the thalamus of rats with SCI-pain we tested the effect of MCS on the activity of neurons in ZI and PO. We demonstrated last year that MCS significantly enhanced spontaneous and evoked responses in the majority of PO-projecting ZI neurons and caused a significant and robust suppression of activity in PO. We now report that inactivation of ZI using muscimol ($GABA_A$ agonist) blocks the effects of MCS stimulation on PO neurons while cutting the pyramidal tracts have no effects on suppressed activity in PO after MCS. These findings further support our overarching hypothesis that MCS alleviates pain by activating the incerto-thalamic pathway.

15. SUBJECT TERMS
Zona Incerta, Posterior Thalamus, Spinal Cord Injury, Pain, Electrical Stimulation

16. SECURITY CLASSIFICATION OF:			**17. LIMITATION OF ABSTRACT**	**18. NUMBER OF PAGES**	**19a. NAME OF RESPONSIBLE PERSON**
a. REPORT	**b. ABSTRACT**	**c. THIS PAGE**			USAMRMC
U	U	U	UU	20	**19b. TELEPHONE NUMBER** *(include area code)*

TABLE OF CONTENTS

INTRODUCTION

A majority of patients develop maladaptive plastic changes within the central nervous system following spinal cord injury. These changes result in abnormal regulation of peripheral inputs, and impaired perception of tactile and painful stimuli. The majority of these patients suffer because conventional treatment fails to reverse these maladaptive changes. An alternative and potentially effective modality of treatment—motor cortex stimulation (MCS)—offers hope for these patients. The goal of the experiments presented in this annual report is to elucidate the neurobiological basis of reduced pain following MCS. We propose that *MCS reverses hyperalgesia by enhancing the activity in the GABAergic nucleus zona incerta (ZI), and therefore inhibiting pain processing in the posterior thalamus (PO).*

In the second year of funding, we focused our efforts on completing the experiments in **Task 1** as outlined in the Statement of Work. The experiments were fruitful and the progress was well within the proposed time line.

Task 1 was to demonstrate that MCS enhances inhibitory inputs from ZI to PO. In this task we proposed to complete 5 subtasks in the first and second year of funding. As proposed in the Statement of Work, **Tasks 1a-c** were completed and their results were included in last year's progress report. In the 2012 report, we include results from **Tasks 1d and 1e. Task 1d** was to demonstrate that pharmacologic inactivation of ZI blocks the effects of MCS on spontaneous and evoked activity of PO neurons; and **Task 1e** was to demonstrate that MCS effects on activity of PO neurons persist after electrolytic lesions of the cortico-spinal tract. We completed these experiment in the proposed time and Task 1 is now fully completed.

BODY

In this project, we test the overarching hypothesis that MCS alleviates hyperalgesia by activating the incerto-thalamic pathway. In the first year of funding, after obtaining approval from the Animal Care and Use Review Office, we demonstrated that MCS enhances activity in PO-rojecting ZI neurons and suppresses activity in the majority of PO neurons. These results (**Tasks 1a-c** in the Statement of Work) were included in last year's Progress Report (2010-2011).

We continue to test our hypothesis and use an model of spinal cord injury (SCI) that recapitulates the clinical characteristics of SCI-pain (Wang and Thompson, 2008; Masri et al., 2009). In this model, we place unilateral electrolytic lesions in the anterolateral quadrant of the spinal cord at the level of C6-T2. These lesions result in diffuse, bilateral mechanical hyperalgesia in the hindpaws approximately 2-3 weeks after injury (see **Detailed Methods**). All the experiments described below were performed in animals with SCI that exhibited frank hyperalgesia.

Task 1d

To demonstrate that pharmacologic inactivation of ZI blocks the effects of MCS on activity of PO neurons (months: 12-18).

In anesthetized animals with SCI-pain we implanted reversible microdialysis probes in ZI and recorded *in vivo* extracellular activity of well-isolated PO neurons (see **Detailed Methods**). We infused muscimol (200 μM, selective $GABA_A$ agonist) into ZI and assessed the responses of PO to 15 minutes of MCS. We stimulated the motor cortex at intensity: 50 μA, frequency: 50 Hz, pulse duration: 300 μs because we found these parameters to be most effective in reducing hyperalgesia and spontaneous pain in our animal model of SCI-pain (Davoody et al., 2011; Lucas et al., 2011).

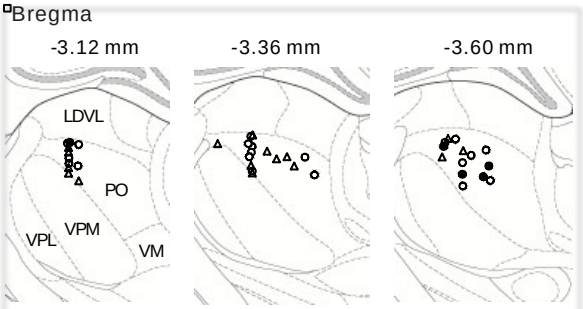

Fig. 1. Postmortem analysis of PO recording sites. Locations of neurons were determined and identified on corresponding drawings obtained from the Paxinos and Watson Atlas (2005). ●: enhanced cell; ○: suppressed cell; Δ: no significant change. Abbreviations: LDVL, laterodorsal thalamic nucleus, ventrolateral part; VPM, ventral posteromedial nucleus; VPL, ventral posterolateral nucleus; VM, ventromedial nucleus.

For each cell in PO (the location of all neurons was confirmed using post-mortem histological analysis, Fig. 1) we recorded: (**1**) Spontaneous activity for at least 5 minutes; (**2**) Responses to noxious and innocuous mechanical stimulation of the receptive field; and (**3**) Spontaneous activity and evoked activity during and immediately after MCS and until the cell recovered. Although we recorded neuronal activity during MCS, we did not include this data in our analysis because the electrical stimulus artifact was large and masked neuronal activity in most instances.

For each individual neuron, the mean firing rate was calculated every minute before and after MCS. Changes in mean firing rate of spontaneous activity over

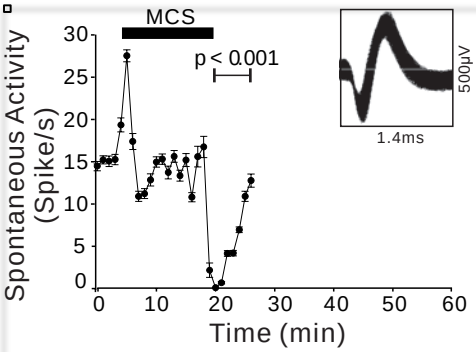

Fig. 2. A representative example of a PO unit suppressed by 15 min of MCS stimulation. Insets represent waveforms of recorded units sorted using a spike matching algorithm. Statistic analysis performed by RM ANOVA).

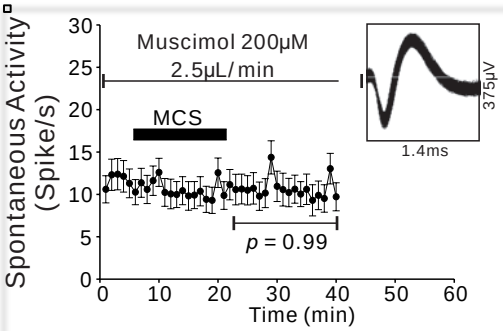

Fig. 3. A representative example of a PO unit exhibiting no change in activity after 15 minutes of MCS (horizontal solid line) when the ZI was inactivated using continuous infusion of muscimol.

time were assessed using Repeated Measures ANOVA when the data was normally distributed and Repeated Measures ANOVA on Ranks when the data was not.. A $p < 0.05$ was considered significant.

We recorded from 47 well-isolated PO cells. In the control group (no inactivation of ZI) 56% (15/27) of the neurons were suppressed following MCS (Range: 1.7%-84.7% suppressed activity; $P<0.05$). In Figure 2 we show a representative example of the effects of MCS on PO activity. MCS suppressed spontaneous activity by 53% after 15 minutes of stimulation (Fig. 2). As expected, the infusion of muscimol blocked the effects of MCS in the majority (73%) of PO neurons studied.

Figure 3 depicts a representative example of a PO neuron where MCS had no effect on spontaneous activity when muscimol was infused in ZI (mean firing rate: 11.7 ± 0.8 spikes/s to 10.7 ± 0.4 spikes/s; $p = 0.987$; RM ANOVA). Taken together these findings suggest that MCS suppresses activity in PO by activating ZI. Summary of the results are provided in Table 1.

Task 1d was completed in the anticipated time and the findings are consistent with our overarching hypothesis that MCS reduces hyperalgesia by activating the incerto-thalamic pathway.

Table 1. The effect of MCS on activity in Po

Experimental Paradigm	Enhanced		Suppressed		No change	
MCS	11%	(3/27)	56%	(15/27)	33%	(9/27)
MCS+ZI Inactivation	0%	(0/20)	75%	(15/20)	25%	(5/20)

Task 1e

To demonstrate that MCS effects on activity of PO neurons persist after electrolytic lesions of the cortico-spinal tract (months: 18-24).

It has been suggested that MCS directly inhibits nociceptive neurons in the dorsal horn (Lindblom and Ottosson, 1957; Andersen et al., 1962) and therefore, suppressed activity in PO could be due to MCS inhibition of ascending nociceptive inputs from the spinal cord rather than due to enhanced ZI activity after MCS. To allay this concern, we performed bilateral pyramidotomy at the level of the caudal medulla (see **Detailed Methods**) and recorded PO responses to 15 minutes of MCS. Cutting the pyramidal tract did not block the effects of MCS and activity of the majority (75%) of PO neurons was suppressed after stimulation. A representative example is shown in Figure 4 where spontaneous activity was significantly suppressed from a mean of 2.5 ± 0.2 spikes/s to 0.2 ± 0.0 spikes/s after 15 minutes of MCS ($p < 0.001$; RM ANOVA). These findings suggest that MCS effects are not due to direct effects of MCS on ascending spinal afferents.

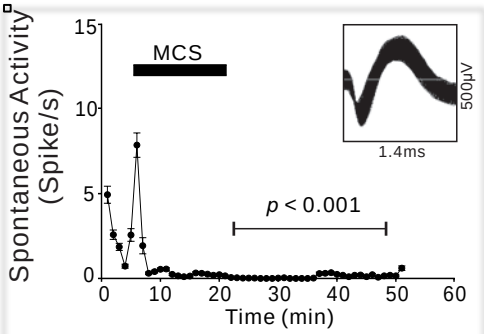

Fig. 4. A representative example of a PO unit exhibiting suppressed activity after 15 minutes of MCS (horizontal solid line) when the pyramidal tract was cut.

In our application, we proposed to cut the pyramidal tract using electrolytic lesions. However, in our initial experiment, we found that these lesions frequently missed the pyramidal tract and even when they were on target, they only produced incomplete cuts. Because of this, we modified our methods to surgically cut the pyramidal tract (see **Detailed Methods**). This produced complete cuts and proved to be more effective.

We completed **Task 1e** within the timeline proposed in the Statement of Work. The result of this task further supports our hypothesis that MCS alleviates hyperalgesia by activating the incertothalamic pathway. We are continuing our experiments and started working on the tasks proposed in our third year of funding. In addition, we are currently compiling all the data that resulted from Task 1 and plan to submit the results for publication in a peer-reviewed journal.

Detailed Methods

Spinal cord lesion. Under aseptic conditions, and using ketamine/xylazine anesthesia (80/10 mg/kg, i.m), a laminectomy to expose the spinal cord between C6 and T2 was performed and the dura was removed. A metal electrode (5 μm tip) was targeted to the anterolateral quadrant in one side of the spinal cord. Current (10 μA for 40 sec) was passed through the electrode to produce an electrolytic lesion. The muscles and skin were sutured in layers to approximate the incision sites. The location of the spinal lesions was assessed after the completion of the experiment in all the animals using postmortem histological analysis.

Behavioral testing. The animals were habituated for two weeks before behavioral testing. Mechanical and thermal hyperalgesia for animals was tested on three consecutive days before the spinal lesion surgery, at day 3 post-surgery, at day 7 post-surgery, and at weekly intervals thereafter as described in (Lucas et al., 2011).

***In vivo* recording in anesthetized animals.** At least 21 days after spinal lesion surgery, animals with confirmed SCI-pain were anesthetized with an intra-peritoneal injection of urethane (1.5 g/kg). The bone overlying the contralateral M1 and the thalamus (in relation to the spinal lesion site) was removed. Extracellular unit recordings were performed using quartz-insulated tungsten electrodes (2 to 4 MΩ). The electrodes were advanced based on stereotaxic coordinates to target PO.

Motor Cortex Stimulation. The hindpaw representation within M1 was identified using electrical microstimulation. Once the hindpaw representation is located, epidural bipolar insulated platinum electrodes (diameter: 70μm, exposed tip: 50μm, distance between the electrodes: 500μm) was secured using skull screws and cemented using dental resin. These electrodes were used for MCS.

Pharmacologic inactivation of ZI. A microdialysis probe (CMA11, Microdialysis, Solna, Sweden) was implanted into ZI using stereotaxic coordinates (Paxinos and Watson, 2005). Muscimol (200 μM, $GABA_A$ agonist; Sigma-Aldrich, Saint Louis, MO, USA) was infused using a pump (Genie Plus, Kent Scientific, CT, USA) at a rate of 2.5 μL / min into ZI 10 minutes before recording from neurons in PO because we found that muscimol infusion requires at least 5 minutes to produce behavioral effects (Lucas et al., 2011)

Pyramidotomy. The pyramidal tract was cut bilaterally at the level of the medulla oblongata before recording from PO neurons to remove any influence of MCS on ascending afferents in the spinal cord. In these animals, the bone covering the medullary pyramids was removed and the dura was dissected. The pyramids were cut 1.5 mm rostral to decussation with a #11 scalpel (Butler Schein, Albany, NY, USA) as described in Z'Graggen et al.,(1998).

Histology. To identify recording sites, at the end of the experiments, we made electrolytic lesions (5 μA for 10 sec), and then deeply anesthetized the rats with sodium pentobarbital (60 mg/kg). The rats were perfused transcardially with buffered saline followed by 4% buffered paraformaldehyde. We obtained coronal brain sections (70 μm thick) and Nissl-stained them. The sections were examined under the microscope to identify recording tracts, lesion sites and stimulating electrodes location.

KEY RESEARCH ACCOMPLISHMENTS

The following is a list of the key research accomplishments during the second year of funding in this project:

- We demonstrated that inactivation of ZI blocks the effects of MCS on PO neurons (**Task 1d**).
- We demonstrated that the effects of MCS on PO neurons remain when the pyramidal tract was cut (**Task 1e**).
- These findings, together with findings from the first year of funding, support the hypothesis that MCS alleviate hyperalgesia by activating the incertothalamic pathway.

REPORTABLE OUTCOMES

1. Publications in peer reviewed Journals
    - Xu S, Ji Y, Chen X, Yang Y, Gullapalli RP, Masri R (2012) In vivo high-resolution localized (1) H MR spectroscopy in the awake rat brain at 7 T. Magn Reson Med. In press.
2. Book Chapters
    - Masri R, Keller A (2012) Chronic pain following spinal cord injury. In: Regenerative biology of the spine and spinal cord (Jandial R, Chen MY, eds), pp 74–85. Austin: Landes Biosciences.
3. Abstracts
    - Mechanisms of Pain Relief Following Motor Cortex Stimulation: An fMRI Study. Society for Neuroscience Meeting. Washington, DC. 2012.
    - Mechanisms of Spinal Cord Injury Pain: A Longitudinal Magnetic Resonance Spectroscopy Study. Society for Neuroscience Meeting. Washington, DC. 2012.
    - Resting State fMRI in a Rat Model of Spinal Cord Injury Neuropathic Pain: A Longitudinal Study. Society for Neuroscience Meeting. Washington, DC. 2012.
    - Mediodorsal Thalamus: Response Properties In Normal and Spinal Cord Injured Rats. Society for Neuroscience Meeting. Washington, DC. 2012.
4. Meetings
    - Attended the 2011 Society for Neuroscience Annual Meeting. Washington, DC.

CONCLUSION

In this report we provide evidence that MCS suppresses activity of PO neurons by enhancing activity in the ZI in animals with SCI-pain. These findings are exciting; they are consistent with our overarching hypothesis that MCS alleviates pain by activating the incerto-thalamic circuit.

The findings of this study describe for the first time a novel pathway that is responsible for the amelioration of SCI-pain. In the coming year, we will continue to investigate this pathway to demonstrate a casual relationship between the suppression of activity in PO and MCS effects on ZI and that these neurophysiological changes can explain the reduction in hyperalgesia and pain after MCS.

REFERENCES

Andersen P, Eccles JC, Sears TA (1962) Presynaptic inhibitory action of cerebral cortex on the spinal cord. Nature 194:740–741.

Davoody L, Quiton RL, Lucas JM, Ji Y, Keller A, Masri R (2011) Conditioned place preference reveals tonic pain in an animal model of central pain. J Pain 12:868–874.

Lindblom UF, Ottosson JO (1957) Influence of pyramidal stimulation upon the relay of coarse cutaneous afferents in the dorsal horn. Acta Physiol Scand 38:309–318.

Lucas JM, Ji Y, Masri R (2011) Motor cortex stimulation reduces hyperalgesia in an animal model of central pain. Pain 152:1398–1407.

Paxinos G, Watson C (2005) The rat brain in stereotaxic coordinates. Academic Press: San Diego.

Z'Graggen WJ, Metz GA, Kartje GL, Thallmair M, Schwab ME (1998) Functional recovery and enhanced corticofugal plasticity after unilateral pyramidal tract lesion and blockade of myelin-associated neurite growth inhibitors in adult rats. J Neurosci 18:4744–4757.

APPENDIX

NOTE

Magnetic Resonance in Medicine 000:000–000 (2012)

In Vivo High-Resolution Localized ^{1}H MR Spectroscopy in the Awake Rat Brain at 7 T

Su Xu,[1,2] Yadong Ji,[3] Xi Chen,[4] Yihong Yang,[4] Rao P. Gullapalli,[1,2] and Radi Masri[3]*

In vivo localized high-resolution ^{1}H MR spectroscopy was performed in multiple brain regions without the use of anesthetic or paralytic agents in awake head-restrained rats that were previously trained in a simulated MRI environment using a 7T MR system. Spectra were obtained using a short echo time single-voxel point-resolved spectroscopy technique with voxel size ranging from 27 to 32.4 mm^3 in the regions of anterior cingulate cortex, somatosensory cortex, hippocampus, and thalamus. Quantifiable spectra, without the need for any additional postprocessing to correct for possible motion, were reliably detected including the metabolites of interest such as γ-aminobutyric acid, glutamine, glutamate, *myo*-inositol, *N*-acetylaspartate, taurine, glycerophosphorylcholine/phosphorylcholine, creatine/phosphocreatine, and *N*-acetylaspartate/*N*-acetylaspartylglutamate. The spectral quality was comparable to spectra from anesthetized animals with sufficient spectral dispersion to separate metabolites such as glutamine and glutamate. Results from this study suggest that reliable information on major metabolites can be obtained without the confounding effects of anesthesia or paralytic agents in rodents. Magn Reson Med 000:000–000, 2012.

Key words: awake; ^{1}H localized MR spectroscopy; brain; high resolution

INTRODUCTION

In vivo high-resolution proton magnetic resonance spectroscopy (^{1}H MRS) has been used extensively to simultaneously measure the concentration of a large number of neurometabolites in normal and diseased brains of human and animals (1–9). Unlike human MRS studies that can be readily performed in conscious participants, in vivo animal MRS is typically performed under anesthesia to keep the animal from moving during data acquisition.

It is well documented that neuronal activity, basal cerebral blood flow, hemodynamic coupling, and blood-oxygenation-level-dependent based signals can be altered by anesthetics or paralytic agents (10–15). Several functional magnetic resonance imaging protocols using awake animals have been developed to circumvent these problems in primates (16–19), rats (14,15,20–26), mice (27), and rabbits (28).

A number of in vivo MRS studies demonstrated that anesthesia affects cerebral metabolic profiles in rats (29–32). These studies suggested that different anesthetics (isoflurane, propofol, and pentobarbital) result in different brain metabolic profiles of glutamate (29), lactate, and glucose (29–32). To the best of our knowledge, only one study investigated neurometabolic profiles using high-resolution localized ^{1}H MRS in awake non-human primates (33). An awake MRS preparation that uses rodents is still lacking despite the extensive use of rodents in basic and translational neuroscience research. The goals of this study were (a) to develop a protocol to perform MRS experiments in awake rats and (b) to determine whether metabolic profiles in various regions of the rat brain can be measured reliably at 7 T in awake, head-restrained preparations using high-resolution ^{1}H MRS. To our knowledge, this is the first report of high-resolution ^{1}H MRS in awake rats.

METHODS

Five female Sprague–Dawley rats (22 days old) were obtained from Harlan Laboratories (Raleigh, NC) and were group housed in standard cages in a 12:12 light/dark cycle with access to food and water ad libitum. All procedures performed on the animals were in strict accordance with the National Institutes of Health *Guide for Care and Use of Laboratory Animals* and approved by the University of Maryland Baltimore College of Dental Surgery, Institutional Animal Care and Use Committee.

Animal Training and Acclimation

To train and acclimate the animals to the MRI environment, we used methods similar to those described in King et al. (23), with some modifications. The animals were acclimated and trained daily to go into a loose-fitting restraining cloth and placed in a custom made plastic replica of the animal bed/holder used in the scanner. During handling and acclimation, the animals initially were restrained for a period of 5 min. The period of restraint was increased gradually and reached a maximum of 30 min toward the end of the training period. During the training, the animals were exposed to tape

[1]Department of Diagnostic Radiology and Nuclear Medicine, University of Maryland School of Medicine, Baltimore, Maryland, USA.
[2]Core for Translational Research in Imaging at Maryland, University of Maryland School of Medicine, Baltimore, Maryland, USA.
[3]Department of Endodontics, Prosthodontics and Operative Dentistry, University of Maryland Dental School, Baltimore, Maryland, USA.
[4]Neuroimaging Research Branch, National Institute on Drug Abuse, National Institutes of Health, Baltimore, Maryland, USA.

Grant sponsor: National Institute of Neurological Disorders and Stroke; Grant number: R01-NS069568 (to R.M.); Grant sponsor: Department of Defense; Grant number: SC090126 (to R.M.).

*Correspondence to: Radi Masri, D.D.S., M.S., Ph.D., Department of Endodontics, Prosthodontics and Operative Dentistry, University of Maryland Dental School, 650 W Baltimore St. Office #6253, Baltimore, MD 21201.
E-mail: radi.masri@gmail.com

Received 23 January 2012; revised 10 April 2012; accepted 11 April 2012.
DOI 10.1002/mrm.24321
Published online in Wiley Online Library (wileyonlinelibrary.com).

recordings of the sound bursts generated by gradient switching in the magnet during MRS experiments. The animals were trained daily until they reached adulthood (~2 months) and by the end of the training period, the rats learned to remain calm in the replica of the scanner holder. After training, the animals were prepared for surgery to attach a custom designed plastic head holder to allow for further head restraint.

Holder Implantation Surgery

The animals were anesthetized with 2% isoflurane, attached to a stereotaxic frame and placed on a thermoregulated heating pad. Depth of anesthesia was determined every 15 min by monitoring pinch withdrawal, eyelid reflex, corneal reflex, respiration rate, and vibrissae movements. Incision sites were injected with local anesthetic (0.5% marcaine) to further reduce the possibility that animals would experience pain. A midline incision overlying the skull extending from the inion to lambda (10 mm) was made using a #11 scalpel blade. The scalp was reflected laterally and six predetermined atraumatic openings were prepared using a pin vise and #66 drill bit (Plastic One Inc., VA). The locations of these openings were as follows: two anterior in the frontal bone, two posterior in the occipital bone, and two bilateral in the parietal bone. Six polyetheretherketone screws (PEEK, 1.7 × 4 mm^2, NetMotion, CA) were used to attach a custom made acrylic resin plastic head holder (Jet Acrylic Resin, Dentsply, PA) to the skull. The acrylic head holder was oval in shape (3-mm thick) with two lateral extensions (15-mm long and 4-mm thick) and fit the calvarium of the rat intimately. The lateral extensions were used to restrain the animal during MRS experiments (Fig. 1a). At the end of surgery, the skin edges were approximated and sutured. During recovery, the animals were placed on a thermoregulated heat pad and observed every 15 min until they recovered completely and monitored daily thereafter. After surgery, buprenorphine HCl (0.01–0.05 mg/kg s.c.) was administered every 12 h for 48 h to reduce pain and discomfort.

One week after surgery, the animals were reintroduced to the replica of the scanner holder. For a period of 7 days, the animals were trained to be restrained using the implanted head mount by attaching the lateral extensions to the scanner replica using plastic screws. The rats cooperated and there was no difficulty positioning them in the restrainer. No food and water were given to the animals during the periods of restraint. However, they were rewarded with a treat (Cheerios® and Froot Loops®) after every restraining session.

MRS Experiment

In vivo MRS experiments were performed on a Bruker BioSpec 70/30USR Avance III 7T horizontal bore MR scanner (Bruker Biospin MRI GmbH, Germany) equipped with a BGA12S gradient system capable of producing pulse gradients of 400 mT/m in each of the three orthogonal axes and interfaced to a Bruker Paravision 5.1 console. A Bruker four-element ^1H surface coil array was used as the receiver and a Bruker 72 mm linear-volume coil as the transmitter. During the spectroscopy experiments, the animals were placed and restrained in the scanner bed in a manner similar to the one in which they were trained. An MR-compatible small-animal monitoring system was used to monitor animal respiration rate continuously through the entire experiment (SA Instruments, Inc., NY). Screen snapshot was taken approximately every 30 min to record both the breathing waveforms and the respiration rate. A three-slice (axial, midsagittal, and coronal) scout using fast low angle shot MRI was obtained to localize the rat brain (34,35). A fast shimming procedure (FASTMAP) was used to improve the B_0 homogeneity for each voxel (36). T_2-weighted MR images covering the entire brain were obtained using a two-dimensional rapid acquisition with relaxation enhancement sequence (37) with repetition time/effective echo time (TR/TE_{eff}) = 4500/28 ms, echo train length = 4, field of view = 3.5 × 3.5 cm^2, matrix size = 256 × 256, slice thickness = 1 mm, and number of averages = 2 for anatomic reference. Four spectroscopy voxels representing regions of interest were selected: anterior cingulate cortex (3 × 3 × 3 mm^3), somatosensory cortex (1.8 × 4.5 × 4.0 mm^3), hippocampus (2.5 × 4.0 × 3.0 mm^3), and the thalamus (3 × 3 × 3 mm^3). For ^1H MRS, adjustments of all first- and second-order shims over the voxel

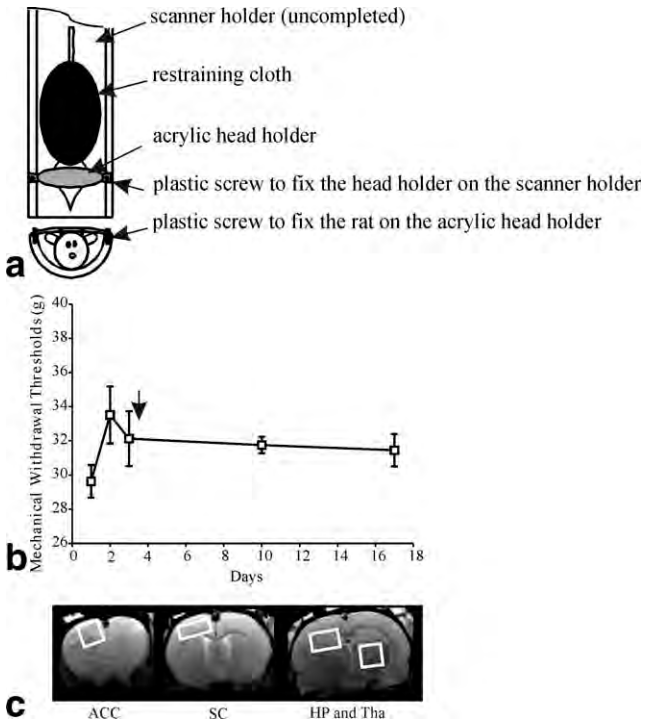

FIG. 1. **a**: Schematic of the experimental setup. A custom made acrylic head holder was used to restrain the rats in the MR scanner. **b**: Mechanical withdrawal thresholds in all the animals was assessed by using an electronic plantar aesthesiometer. Arrow indicate the time of head holder implantation surgery and error bars = standard error of the mean. **c**: The transverse MRIs obtained using rapid acquisition with relaxation enhancement sequence (TR/TE_{eff} = 4500/28 ms) of the brain of awake head-restrained rats. The 4 voxel locations for MRS experiment are highlighted. ACC = anterior cingulate cortex, SC = somatosensory cortex, HP = hippocampus (left), and Tha = thalamus (right).

of interest were accomplished with the FASTMAP procedure. Typically, the in vivo shimming procedure resulted in approximately 13 Hz full-width half maximum line width of the unsuppressed water peak over the spectroscopy voxel. The point-resolved spectroscopy pulse sequence was customized using a sinc7H pulse with a hamming window modulation providing an excitation bandwidth of 10 kHz. Two asymmetric pulses with a bandwidth of 2823 Hz were used for refocusing (38), which corresponds to 32% chemical shift displacement error in two directions for the chemical shift range of 3 ppm. The TE was shortened to 10 ms to alleviate signal attenuations caused by J modulation and T_2 relaxation. The center frequencies of the above three localization pulses were placed at 3.0 ppm to reduce the lipid contamination caused by the chemical shift displacement. This custom made point-resolved spectroscopy sequence (TR/TE = 2500/10 ms, number of average = 356) was used for MRS data acquisition from various regions including anterior cingulate cortex, somatosensory cortex, hippocampus, and thalamus. The acquisition time for each voxel was 15 min. In one animal, the MRS scan was repeated using the same parameters on 2 consecutives days to test for reproducibility of the MRS results.

Behavioral Assessment

Chronic restraint is stressful and the stress has been shown to be associated with reduced mechanical withdrawal thresholds and hyperalgesia in rodents (39,40). Therefore, to test if our acclimation, head-restraint, and MRS procedures produced chronic stress and hyperalgesia, we assessed hindpaw mechanical withdrawal thresholds in all the animals. Mechanical withdrawal thresholds of both hindpaws were assessed in all the animals at: baseline (3 consecutive days before implantation of the head holder); 1 week after the implantation of the head holder; and immediately after each MRS scan. A dynamic planter aesthesiometer (Ugo Basile, PA) was used to determine hindpaw mechanical withdrawal thresholds as described by Dolan and Nolan (41). The nonparametric Friedman test was used to assess if mechanical withdrawal thresholds changed significantly over time. A P value of less than 0.05 was considered significant.

Data Analysis

Quantification of the MRS was based on frequency domain analysis using "Linear Combination of Model spectra" (LCModel) (42). In vivo spectra were analyzed by a superposition of a set of simulated basis set provided by the LCModel software. The reference for determining metabolite concentration was the water signal, which was acquired from the same voxel. The metabolic profile was measured with the same parameters except the number of averages was set at 8. The results were normalized by LCModel package to the metabolite concentrations and expressed as micromoles per gram wet weight (μM). Cramér–Rao lower bounds (CRLB) as reported from the LCModel analysis was used for assessing the reliability of the major metabolites. To provide an indicator of reproducibility, the coefficient of variability (CV) was calculated for the individual metabolites across individual animals as the ratio of the square root of the standard deviation to the mean.

RESULTS

In three of the animals, MRS data were obtained from all four regions. In one animal, MRS data were obtained from three regions (somatosensory cortex, hippocampus, and thalamus). In the fifth animal, MRS data were obtained from anterior cingulate cortex, as this was the first trained animal. Therefore, for the quantitative analysis, four datasets (n = 4) were used in each region although a total of five animals were used in this study.

In all animals, we assessed mechanical withdrawal thresholds to test if chronic restraint resulted in stress and hyperalgesia (39,40). Our training and restraining procedures did not result in any significant change over time in mechanical withdrawal thresholds (P = 0.31, Friedman test; Fig. 1b).

Axial anatomic images along with the four spectroscopic voxel locations including the anterior cingulate cortex, somatosensory cortex, hippocampus, and the thalamus are shown in Fig. 1c. High-resolution localized ^1H MR spectra from the 4 voxels are shown in Fig. 2. In these spectra, a number of metabolites can be reliably detected. *N*-Acetylaspartate (NAA) methyl singlet at 2.01 ppm was assigned as the reference. The line width of the singlet ^1H metabolite resonances (as measured on tCr at 3.0 ppm; Fig. 2) was typically 11–15 Hz (0.037–0.050 ppm) in awake animals and was comparable to the spectra from anesthetized animals (9). The concentrations of the metabolites measured by LCModel from these 4 voxels are listed in Table 1. The reliability of the major metabolites that was estimated by the LCModel using the CRLB is also listed in Table 1. In general, the CRLB values of Glu (3–7%), Ins (5–10%), Tau (6–8%), GPC+PCh (4–7%), NAA+NAAG (3–5%), Cr+PCr (3–5%), and Glx (4–8%) were not more than 10 %. For the low-concentration metabolites γ-aminobutyric acid (GABA; 9–18%) and glutamine (9–15%), the highest CRLB value was 18%. The exceptions are GABA (13–21%), glutamine (17–27%), and Tau (15–29%) levels in the thalamus.

To test the reproducibility of MRS, we repeated the MRS scan in one rat on 2 consecutive days. Figure 2a shows spectra acquired on day-1 from the 4 voxels and Fig. 2b shows spectra acquired from the same rat on day-2. Spectra obtained from the four regions appear to be similar at the two time points. In Table 2, we quantitatively analyze the spectra acquired in the somatosensory cortex (Fig. 2). The coefficient of variation was not more than 11% for all the metabolites considered. These findings suggest that the awake animal MRS is reproducible in the same animal. However, it is important to note that the CV values obtained from only two experiments may not be reliable. In addition, the breathing waveforms and respiration rates of this rat exhibited stable breathing pattern and rate (53–76 breath/min) suggesting minimal stress on the animal during both scans.

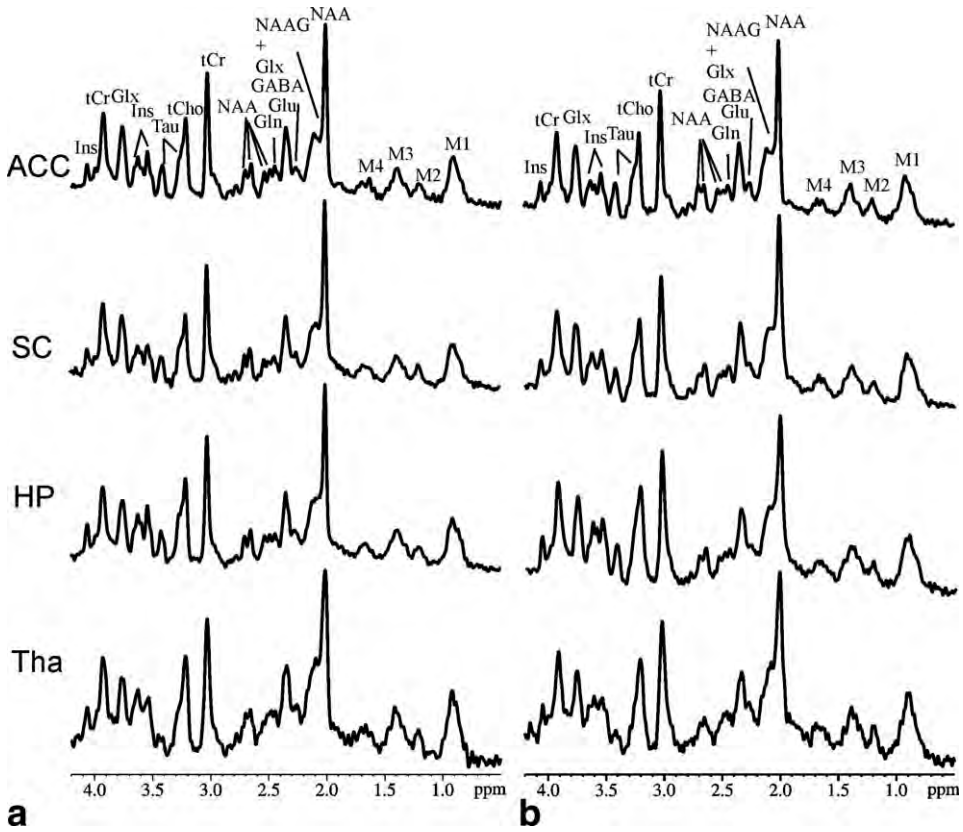

FIG. 2. In vivo ^{1}H short-TE MR spectra from four brain regions of an awake rat acquired at 7 T at with a localized point-resolved spectroscopy sequence (TR/TE = 2500/10 ms) at day-1 (**a**) and day-2 (**b**). The spectrum was phased using zero-order phase only without any baseline corrections. Resolution enhancement was done with Lorentzian–gaussian transformation scheme (lb = −4, gb = 0.15). tCr = total creatine, GABA = γ-aminobutyric acid, Gln = glutamine, Glu = glutamate, Glx = glutamine + glutamate, Ins = *myo*-inositol, NAA = *N*-acetylaspartate, NAAG = *N*-acetylaspartylglutamate, tCho = glycerophosphocholine + phosphocholine, Tau = taurine, M1 = macromolecule at 0.92 ppm, M2 = macromolecule at 1.21 ppm, M3 = macromolecule at 1.39 ppm, M4 = macromolecule at 1.62 ppm. ACC = anterior cingulate cortex, SC = somatosensory cortex, HP = hippocampus, and Tha = thalamus.

DISCUSSIONS AND CONCLUSIONS

In this study, a novel head-restraining system was successfully implemented for the first time to obtain metabolic information using MRS in an awake rodents. Using this preparation, it is possible to obtain localized ^{1}H MR spectra in several brain regions of interest (anterior cingulate cortex, somatosensory cortex, hippocampus, and thalamus) without the need for any postprocessing scheme to correct for possible motion during data acquisition. In all four regions, most brain metabolites or the combinations were reliably detected (CRLB $<$ 18%), except for some metabolites in the thalamus. Because of the use of a surface coil, the rostral regions of the anterior cingulate cortex, somatosensory cortex, and hippocampus exhibited high signal-to-noise ratio (∼22), and the spectra obtained were highly reliable (CRLB $<$ 18%). The overall signal to noise of the spectra for thalamus was lower (∼13), as this region was at the periphery of the reception field of the four-element surface coil. In this region, metabolites with low concentration provided less reliable spectra (GABA, glutamine, and Tau; CRLB = 21–29%; Table 1).

The concentrations of the metabolites quantified in this study are within the range specified in the rat brain (see Table 3 in Ref. 43). It is important to note however that the GABA concentration may be overestimated in this study because there can be a significant overlap with the macromolecules in the GABA region of the spectrum. In addition, the Tau concentration may be underestimated because of its long spin-lattice relaxation time and short TR (44).

The concentrations of metabolites appear to be different from those reported in Xin et al. and Rao et al. (45,46). In our study, MRS experiments were performed in 14-week old female rats to assess metabolic profiles in the somatosensory cortex, anterior cingulate cortex, hippocampus, and the thalamus. In Xin et al. (45), the animal gender was different (adult male rats), and although the regions of interest studied included the somatosensory cortex and hippocampus, the voxel sizes used were significantly different (somatosensory cortex: $6 \times 1.5 \times 2$ mm^3 vs. $1.8 \times 4.5 \times 4.0$ mm^3 in this study; hippocampus: $3 \times 2 \times 2$ mm^3 vs. $2.5 \times 4.0 \times 3.0$ mm^3] (45). In Rao et al. (46), the age and gender of the animals (8-week old, male) were also different. The methodological differences between this study and the studies referenced above may explain the differences in metabolites' concentrations. It is well documented that metabolic profiles depend on the age and gender of the animals as well as the region studied (46–48).

Table 1
Quantitative Analysis of Spectra Acquired in the Four Regions of Interest

	GABA	Gln	Glu	Ins	NAA	Tau	tCho	NAA+NAAG	tCr	Glx
Anterior cingulate cortex										
Mean (μmol/g)	2.72	2.66	9.90	4.78	7.60	4.07	1.21	8.39	5.91	12.55
SE (μmol/g)	0.03	0.24	0.31	0.18	0.11	0.23	0.03	0.12	0.04	0.43
CRLB (%)	9–11	9–13	3–4	5–8	3–4	5–9	4–5	3	3–4	4–5
Somatosensory cortex										
Mean (μmol/g)	2.21	2.31	8.47	4.42	6.91	3.33	0.93	7.79	5.37	10.78
SE (μmol/g)	0.13	0.05	0.50	0.43	0.35	0.11	0.04	0.40	0.22	0.54
CRLB (%)	10–13	12–14	4	5–10	3–4	5–9	5–6	3–4	3–4	4–5
Hippocampus										
Mean (μmol/g)	2.21	2.29	7.75	6.07	6.27	4.35	1.12	6.85	5.65	10.04
SE (μmol/g)	0.20	0.09	0.52	0.20	0.15	0.30	0.07	0.26	0.11	0.59
CRLB (%)	9–18	11–15	4–5	5–6	3–6	6–7	4–5	3–4	3–4	4–6
Thalamus										
Mean (μmol/g)	2.29	1.72	7.88	4.82	7.05	1.91	1.47	7.70	5.78	9.60
SE (μmol/g)	0.13	0.10	0.30	0.32	0.32	0.09	0.11	0.36	0.37	0.26
CRLB (%)	13–21	17–27	5–7	5–10	4–6	15–29	5–7	4–5	4–5	6–8

SE = standard error of the mean; CRLB = Cramér–Rao lower bounds; tCr = total creatine; GABA = γ-aminobutyric acid; Gln = glutamine; Glu = glutamate; Glx = glutamine + glutamate; Ins = *myo*-inositol; NAA = *N*-acetylaspartate; NAAG = *N*-acetylaspartylglutamate; tCho = glycerophosphocholine + phosphocholine; Tau = taurine.

A major concern when performing experiments in restrained animals is the stress induced (39,40,49) and its effect on MRS results. To minimize this concern, we adopted similar methods to those described in King et al. (23) and acclimated and handled the animals from a young age before performing the experiments. We also assessed changes in mechanical withdrawal thresholds over time and monitored breathing during the MRS experiments. The acclimation and training procedure proved effective in reducing animal stress as evident from the lack of change in mechanical withdrawal thresholds and the stable and normal breathing rate. Future experiments should test if awake MRS experiments can be performed using shorter training paradigms as those described in Becerra et al. (50). In addition, the experiments should assess the state of the animal and investigate whether stress was induced or not. Such experiments will benefit from quantifying serum cortisone levels during the imaging procedures and monitoring the heart rate (23,24).

MRS acquisitions require that the main magnetic field, B_0, remains very stable during data acquisition. The movement of the animal during the data acquisition can significantly change the value of the local B_0 over time. B_0 fluctuations can broaden the line width of the observed metabolites in the MR spectrum thereby losing fidelity in resolving two closely resonating spins. In a ^1H MRS study on awake non-human primates at 7 T (33), line width changed from 15.6 Hz at the beginning of the study to 19.5 Hz for the averaged spectrum. These changes in the spectral line width were due to major body movement of the awake animal during data acquisition. However, respiration and small body movement did not show a significant spatial B_0 dependence and shim effect. To correct for movement, the authors applied a scheme that rejected periods of major body motion and corrected frequency/phase of each of the single acquisition of the spectra before averaging (33). Using this correction scheme, the line width of the spectrum was reduced to 15.8 Hz. In our experimental design, a motion correction scheme was not performed. The shimming procedure routinely resulted in line widths of 11–15 Hz of the single ^1H metabolite resonance (0.037–0.050 ppm) and a good separation of peaks that resonate closely was possible (e.g., glutamate [2.35 ppm] and glutamine [2.45 ppm]). Furthermore, repeated acquisition of the spectra over 2 different days were highly reproducible (CV <11%) suggesting that preparing the animal in this manner leads to negligible motion and provides a stable environment for obtaining quality MRS. However,

Table 2
Analysis of Intraindividual Spectra Acquired in Somatosensory Cortex at 2 Consecutive Days

	GABA	Gln	Glu	Ins	NAA	Tau	tCho	NAA+NAAG	tCr	Glx
Day-1										
Concentration (μmol/g)	2.39	2.23	8.43	4.61	7.23	3.65	0.97	8.04	5.26	10.66
CRLB (%)	10	12	4	5	3	5	5	3	3	4
Day-2										
Concentration (μmol/g)	2.80	2.57	8.91	5.78	7.13	3.45	1.12	8.21	5.49	11.48
CRLB (%)	8	10	3	5	3	6	4	3	3	4
CV (%)	8	7	3	11	1	3	7	1	2	4

CRLB = Cramér–Rao lower bounds; CV = coefficient of variability; tCr = total creatine; GABA = γ-aminobutyric acid; Gln = glutamine; Glu = glutamate; Glx = glutamine + glutamate; Ins = *myo*-inositol; NAA = *N*-acetylaspartate; NAAG = *N*-acetylaspartylglutamate; tCho = glycerophosphocholine + phosphocholine; Tau = taurine.

the quality of the raw spectra acquired can be further improved by performing additional data preprocessing steps as those described in Pfeuffer et al. (33). Correcting for animal movement and frequency/phase of single acquisitions will reduce the minimum detectable differences in metabolite concentrations and increase reproducibility and therefore improve the quality of the acquired spectra.

Rodents are used extensively in neuroscience research to study disease processes that involve cognition and emotion such as pain, addiction, depression, and psychiatric disorders. These conditions cannot be studied reliably in the presence of agents that may alter consciousness, cognition, and neuronal transmission. Similarly, MRS has proven very useful in studying the pathophysiologic mechanisms of a large range of neurological and psychiatric disorders (2), and many of these studies are not possible if the animals are not restrained to prevent movement. An awake rodent MRS preparation as demonstrated here allows one to study these conditions and correlate changes in brain metabolic profiles during resting and functional states with changes in neuronal physiology, chemistry, and behavior without the confounds of anesthetic and paralytic agents.

We conclude that high-resolution and high-quality ^{1}H MRS can be obtained from unanesthetized rat brains at 7 T. With proper training and restraint apparatus, several proton metabolites can be reliably measured even without postprocessing correction schemes. The current development offers a novel approach to study major brain metabolites in awake rodents. This method circumvents the effects of anesthesia and allows for longitudinal experiments for prolonged periods of time to study progression of disease especially in the field of chronic pain research. It will also open the door for translational research that bridges the gap between animal and human studies.

ACKNOWLEDGMENTS

This research project was supported by a research grant from the National Institute of Neurological Disorders and Stroke (to R.M.) and research grant from the Department of Defense (to R.M.).

REFERENCES

1. Ross B, Bluml S. Magnetic resonance spectroscopy of the human brain. Anat Rec 2001;265:54–84.
2. Ross AJ, Sachdev PS. Magnetic resonance spectroscopy in cognitive research. Brain Res Brain Res Rev 2004;44:83–102.
3. Soher BJ, Doraiswamy PM, Charles HC. A review of ^{1}H MR spectroscopy findings in Alzheimer's disease. Neuroimaging Clin N Am 2005;15:847–852.
4. Sibtain NA, Howe FA, Saunders DE. The clinical value of proton magnetic resonance spectroscopy in adult brain tumours. Clin Radiol 2007;62:109–119.
5. Choi IY, Lee SP, Guilfoyle DN, Helpern JA. *In vivo* NMR studies of neurodegenerative diseases in transgenic and rodent models. Neurochem Res 2003;28:987–1001.
6. Tkac I, Henry PG, Andersen P, Keene CD, Low WC, Gruetter R. Highly resolved *in vivo* ^{1}H NMR spectroscopy of the mouse brain at 9.4 T. Magn Reson Med 2004;52:478–484.
7. Xu S, Yang J, Li CQ, Zhu W, Shen J. Metabolic alterations in focally activated primary somatosensory cortex of alpha-chloralose-anesthetized rats measured by ^{1}H MRS at 11.7 T. Neuroimage 2005;28:401–409.
8. Mlynarik V, Cudalbu C, Xin L, Gruetter R. ^{1}H NMR spectroscopy of rat brain in vivo at 14.1Tesla: improvements in quantification of the neurochemical profile. J Magn Reson 2008;194:163–168.
9. Xu S, Zhuo J, Racz J, Shi D, Roys S, Fiskum G, Gullapalli R. Early microstructural and metabolic changes following controlled cortical impact injury in rat: a magnetic resonance imaging and spectroscopy study. J Neurotrauma 2011;28:2091–2102.
10. Ueki M, Mies G, Hossmann KA. Effect of alpha-chloralose, halothane, pentobarbital and nitrous oxide anesthesia on metabolic coupling in somatosensory cortex of rat. Acta Anaesthesiol Scand 1992;36:318–322.
11. Bonvento G, Charbonne R, Correze JL, Borredon J, Seylaz J, Lacombe P. Is alpha-chloralose plus halothane induction a suitable anesthetic regimen for cerebrovascular research? Brain Res 1994;665:213–221.
12. Lahti KM, Ferris CF, Li F, Sotak CH, King JA. Comparison of evoked cortical activity in conscious and propofol-anesthetized rats using functional MRI. Magn Reson Med 1999;41:412–416.
13. Nakao Y, Itoh Y, Kuang TY, Cook M, Jehle J, Sokoloff L. Effects of anesthesia on functional activation of cerebral blood flow and metabolism. Proc Natl Acad Sci USA 2001;98:7593–7598.
14. Sicard K, Shen Q, Brevard, ME, Sullivan R, Ferris CF, King JA, Duong TQ. Regional cerebral blood flow and BOLD responses in conscious and anesthetized rats under basal and hypercapnic conditions: implications for functional MRI studies. J Cereb Blood Flow Metab 2003;23:472–481.
15. Martin C, Jones M, Martindale J, Mayhew J. Haemodynamic and neural responses to hypercapnia in the awake rat. Eur J Neurosci 2006;24:2601–2610.
16. Stefanacci L, Reber P, Costanza J, Wong E, Buxton R, Zola S, Squire L, Albright T. fMRI of monkey visual cortex. Neuron 1998;20:1051–1057.
17. Logothetis NK, Guggenberger H, Peled S, Pauls J. Functional imaging of the monkey brain. Nat Neurosci 1999;2:555–562.
18. Meyer JS, Brevard ME, Piper BJ, Ali SF, Ferris, CF. Neural effects of MDMA as determined by functional magnetic resonance imaging and magnetic resonance spectroscopy in awake marmoset monkeys. Ann N Y Acad Sci 2006;1074:365–376.
19. Stoewer S, Goense J, Keliris GA, Bartels A, Logothetis NK, Duncan J, Sigala N. Realignment strategies for awake-monkey fMRI data. Magn Reson Imaging 2011;29:1390–1400.
20. Lahti KM, Ferris CF, Li F, Sotak CH, King JA. Imaging brain activity in conscious animals using functional MRI. J Neurosci Methods 1998;82:75–83.
21. Tabuchi E, Yokawa T, Mallick H, Inubushi T, Kondoh T, Ono T, Torii K. Spatio-temporal dynamics of brain activated regions during drinking behavior in rats. Brain Res 2002;951:270–279.
22. Sachdev RNS, Champney GC, Lee H, Price RR, Pickens DR III, Morgan VL, Stefansic JD, Melzer P, Ebner FF. Experimental model for functional magnetic resonance imaging of somatic sensory cortex in the unanesthetized rat. Neuroimage 2003;19:742–750.
23. King JA, Garelick TS, Brevard ME, Chen W, Messenger TL, Duong TQ, Ferris CF. Procedure for minimizing stress for fMRI studies in conscious rats. J Neurosci Methods 2005;148:154–160.
24. Becerra L, Pendse G, Chang PC, Bishop J, Borsook D. Robust reproducible resting state networks in the awake rodent brain. PLoS One 2011;6:e25701.
25. Liang Z, King J, Zhang N. Uncovering intrinsic connectional architecture of functional networks in awake rat brain. J Neurosci 2011;31:3776–3783.
26. Liang Z, King J, Zhang N. Anticorrelated resting-state functional connectivity in awake rat brain. Neuroimage 2012;59:1190–1199.
27. Desai M, Kahn I, Knoblich U, Bernstein J, Atallah H, Yang A, Kopell N, Buckner RL, Graybiel AM, Moore CI. Mapping brain networks in awake mice using combined optical neural control and fMRI. J Neurophysiol 2011;105:1393–1405.
28. Wyrwicz AM, Chen N, Li L, Weiss C, Disterhoft JF. fMRI of visual system activation in the conscious rabbit. Magn Reson Med 2000;44:474–478.
29. Makaryus R, Lee H, Yu M, Zhang S, Smith SD, Rebecchi M, Glass PS, Benveniste H. The metabolomic profile during isoflurane anesthesia differs from propofol anesthesia in the live rodent brain. J Cereb Blood Flow Metab 2011;31:1432–1442.
30. Choi IY, Lei H, Gruetter R. Effect of deep pentobarbital anesthesia on neurotransmitter metabolism *in vivo*: on the correlation of total glucose consumption with glutamatergic action. J Cereb Blood Flow Metab 2002;22:1343–1351.

31. Du F, Zhang Y, Iltis I, Marjanska M, Zhu XH, Henry PG, Chen W. *In vivo* proton MRS to quantify anesthetic effects of pentobarbital on cerebral metabolism and brain activity in rat. Magn Reson Med 2009; 62:1385–1393.
32. Lei H, Duarte JM, Mlynarik V, Python A, Gruetter R. Deep thiopental anesthesia alters steady-state glucose homeostasis but not the neurochemical profile of rat cortex. J Neurosci Res 2010;88: 413–419.
33. Pfeuffer J, Juchem C, Merkle H, Nauerth A, Logothetis NK. High-field localized ^1H NMR spectroscopy in the anesthetized and in the awake monkey. Magn Reson Imaging 2004;22:1361–1372.
34. Frahm J, Haase A, Matthaei D. Rapid three-dimensional MR imaging using the FLASH technique. J Comput Assist Tomogr 1986;10: 363–368.
35. Haase A, Frahm J, Matthaei D, Hanicke W, Merboldt KD. FLASH imaging. Rapid NMR imaging using low flip-angle pulses. J Magn Reson 1986;67:258–266.
36. Gruetter R. Automatic, Localized *in vivo* adjustment of all first- and second- order shim coils. Magn Reson Med 1993;29:804–811.
37. Hennig J, Nauerth A, Friedburg H. RARE imaging: a fast imaging method for clinical MR. Magn Reson Med 1986;3:823–833.
38. Mao J, Mareci TH, Andrew ER. Experimental study of optimal selective 180 radiofrequency pulses. J Magn Reson 1988;79:1–10.
39. Porro CA, Carli G. Immobilization and restraint effects on pain reactions in animals. Pain 1988;32:289–307.
40. Rivat C, Laboureyras E, Laulin JP, Le Roy C, Richebé P, Simonnet G. Non-nociceptive environmental stress induces hyperalgesia, not analgesia, in pain and opioid-experienced rats. Neuropsychopharmacology 2007;32:2217–2228.
41. Dolan S, Nolan AM. Blockade of metabotropic glutamate receptor 5 activation inhibits mechanical hypersensitivity following abdominal surgery. Eur J Pain 2007;11:644–651.
42. Provencher SW. Automatic quantitation of localized *in vivo* ^1H spectra with LCModel. NMR Biomed 2001;14:260–264.
43. Pfeuffer J, Tkác I, Provencher SW, Gruetter R. Toward an *in vivo* neurochemical profile: quantification of 18 metabolites in short-echo-time (1)H NMR spectra of the rat brain. J Magn Reson 1999;141:104–120.
44. Cudalbu C, Mlynárik V, Xin L, Gruetter R. Comparison of T_1 relaxation times of the neurochemical profile in rat brain at 9.4 Tesla and 14.1 Tesla. Magn Reson Med 2009;62:862–867.
45. Xin L, Gambarota G, Duarte JM, Mlynárik V, Gruetter R. Direct *in vivo* measurement of glycine and the neurochemical profile in the rat medulla oblongata. NMR Biomed 2010;23:1097–1102.
46. Rao R, Tkac I, Schmidt AT, Georgieff MK. Fetal and neonatal iron deficiency causes volume loss and alters the neurochemical profile of the adult rat hippocampus. Nutr Neurosci 2011;14:59–65.
47. O'Gorman RL, Michels L, Edden RA, Murdoch JB, Martin E. *In vivo* detection of GABA and glutamate with MEGA-PRESS: reproducibility and gender effects. J Magn Reson Imaging 2011;33:1262–1267.
48. Tkác I, Rao R, Georgieff MK, Gruetter R. Developmental and regional changes in the neurochemical profile of the rat brain determined by *in vivo* 1H NMR spectroscopy. Magn Reson Med 2003;50:24–32.
49. Bauer ME, Perks P, Lightman SL, Shanks N. Restraint stress is associated with changes in glucocorticoid immunoregulation. Physiol Behav 2001;73:525–532.
50. Becerra L, Chang PC, Bishop J, Borsook D. CNS activation maps in awake rats exposed to thermal stimuli to the dorsum of the hindpaw. Neuroimage 2011;54:1355–1366.